Cardiac electrical activity imaging of patients with CRBBB or CLBBB in magnetocardiography*

Zhu Jun-Jie(朱俊杰)[a], Jiang Shi-Qin(蒋式勤)[a]†, Wang Wei-Yuan(王伟远)[a], Zhao Chen(赵 晨)[a], Wu Yan-Hua(吴燕华)[a], Luo Ming(罗 明)[b], and Quan Wei-Wei(权薇薇)[c]

[a] *Department of Control Science and Engineering, School of Electronics and Information Engineering, Tongji University, Shanghai* 201804, *China*
[b] *Department of Cardiology of Tongji Hospital Affiliated to Tongji University Medical School, Shanghai* 200065, *China*
[c] *Department of Cardiology of Ruijin Hospital Affiliated to Jiaotong University Medical School, Shanghai* 200025, *China*

(Received 7 September 2013; revised manuscript received 5 November 2013; published online 20 February 2014)

A new method for the imaging of cardiac electrical activity in patients with complete right bundle branch block (CRBBB) or complete left bundle branch block (CLBBB) is investigated using magnetocardiographic recordings of the surface of the body. This is based on the assumption that an equivalent single-current dipole moves along the unblocked bundle branch, whose position in the measurement plane is expressed in terms of the maximum and minimum, as well as the maximum gradient value of the measured magnetic field. The trajectory of the moving dipole on the measurement plane is indicative of the excitation conduction of the CRBBB or CLBBB subject during ventricular depolarization and repolarization, which is deduced by comparing each change between the dipole moment and the maximum current density in a corresponding pseudo-current density map. In summary, this method can distinguish CRBBB from CLBBB subjects by means of the dipole depth and two dipole moment components. The possibility of visualizing the excitation conduction in a CRBBB or CLBBB subject during ventricular depolarization and repolarization is then discussed.

Keywords: biomagnetism, inverse problem, magnetocardiography (MCG), current source reconstruction (CSR), CRBBB or CLBBB

PACS: 87.85.–d, 87.85.Pq, 87.85.Tu, 87.85.Ng **DOI:** 10.1088/1674-1056/23/4/048702

1. Introduction

Since the emergence of superconducting quantum interference devices (SQUIDs), which allow weak cardiac magnetic signals to be detected over a subject's body surface, a new technique known as magnetocardiography (MCG)[1–3] has aroused considerable interest among scientists. MCG has been investigated with the aim of estimating cardiac dipoles and visualizing cardiac electric activity, and noninvasively diagnosing heart disease.

Previous studies have attempted to solve electrocardiography (ECG) inverse problems by seeking the generators of body surface potential maps (BSPMs), since BSPMs are the manifestation of cardiac electric sources on the surface of the body.[4–8] Thenceforth, equivalent dipole solutions were investigated with the aim of functional source localization in electrocardiograms or magnetocardiograms.[9–11]

In recent decades, the reconstruction of the current dipole of the cardiac magnetic field has been studied using the distributed source model[12–15] or the current multipole model,[16,17] whereby the intracellular current is approximated as a set of equivalent dipoles with fixed positions in the heart. The use of distributed source solutions not only overcomes the ill-posed problem in source parameter calculations, but also has the ability to extract local information about cardiac electrical activity on the surface of the heart or in a three-dimensional myocardium. However, visualizing cardiac electrical activity in the spatiotemporal domain still remains a great challenge in clinical applications.

In this study, the cardiac electrical activities of patients with complete right bundle branch block (CRBBB) and complete left bundle branch block (CLBBB) are investigated based on the solution of equivalent single current dipole and bipolar magnetocardiograms. An assumption is made that the equivalent current dipole is always located at the point where the maximum gradient exists in the magnetocardiogram.[13] The dipole moves along the unblocked bundle branch that is indicative of the propagation of the electrical excitation in the heart. The dipole parameters are expressed in the form of the maximum value of the field and the maximum gradient value of the field in an MCG map, as a visual aid.[18]

In Section 2 of this paper, the solution of an equivalent single-current dipole is described. In Section 3, the calculated results of two sets of MCG data from CRBBB and CLBBB subjects are shown, and in Section 4, a comparison of this

*Project supported in part by the National Natural Science Foundation of China (Grant No. 60771030), the National High-Technology Research and Development Program of China (Grant No. 2008AA02Z308), the Shanghai Science and Technology Development Foundation (Grant No. 08JC1421800), the Shanghai Leading Academic Discipline Project (Grant No. B004), the Open Project of State Key Laboratory of Function Materials for Information (Shanghai Institute of Microsystem and Information Technology, Chinese Academy of Sciences), and the Key Laboratory of Medical Imaging Computing and Computer Assisted Intervention of Shanghai (Grant No. 13DZ2272200-2).

†Corresponding author. E-mail: sqjiang@tongji.edu.cn

© 2014 Chinese Physical Society and IOP Publishing Ltd

method with the pseudo-current density (PCD) map is given. The possibility of visualizing the excitation conduction in a CRBBB or CLBBB subject during ventricular depolarization and repolarization is discussed. Section 5 is the conclusion.

2. Model and method

2.1. Inverse solution

Based on quasi-static approximation of the Maxwell equations, the magnetic induction $B(\boldsymbol{r})$ is given by the Biot–Savart law[18]

$$B(\boldsymbol{r}) = \frac{\mu_0}{4\pi}\int_G J(\boldsymbol{r}') \times \frac{\boldsymbol{r}-\boldsymbol{r}'}{|\boldsymbol{r}-\boldsymbol{r}'|^3}\,\mathrm{d}\upsilon', \tag{1}$$

where the field $B(\boldsymbol{r})$ outside the volume conductor G with the permeability of the vacuum μ_0 is determined by the total current density $J(\boldsymbol{r}')$ and the properties of the volume conductor. The z component of $B(\boldsymbol{r})$ perpendicular to a measurement plane outside of the volume conductor, i.e., field B_z produced by a single equivalent current dipole can be expressed in Cartesian coordinates as

$$B_z = \frac{\mu_0}{4\pi}\cdot\frac{(y-y_0)Q_x-(x-x_0)Q_y}{((x-x_0)^2+(y-y_0)^2+z_0^2)^{3/2}}, \tag{2}$$

where $(x_0,\ y_0,\ z_0)$ is the location of the equivalent current dipole. Q_x and Q_y denote two components of the dipole moment.

The modulus of the gradient vector of field B_z is of the form

$$M = \sqrt{\left(\frac{\partial B_z}{\partial x}\right)^2+\left(\frac{\partial B_z}{\partial y}\right)^2}. \tag{3}$$

The point at which the maximum or minimum of M exists can be found by setting the derivative of M to zero as $\partial M/\partial x = \partial M/\partial y = 0$.

We have from Eq. (2) that

$$\begin{cases} \dfrac{\partial B_Z}{\partial x} = \mu_0\cdot\{3(x-x_0)(y-y_0)Q_x \\ \qquad\qquad +[(y-y_0)^2+z_0^2-2(x-x_0)^2]Q_y\}/4\pi = 0, \\ \dfrac{\partial B_Z}{\partial y} = \mu_0\cdot\{[(x-x_0)^2+z_0^2-2(y-y_0)^2]Q_x \\ \qquad\qquad +3(x-x_0)(y-y_0)Q_y\}/4\pi = 0. \end{cases} \tag{4}$$

Equation (4) implies

$$(x-x_0)^2+(y-y_0)^2 = z_0^2/2. \tag{5}$$

That is, the dipole parameter $(x_0,y_0,z_0;Q_x,Q_y)$ in Eq. (2) can be determined by Eqs. (2), (4), and (5), as shown in Eq. (6).

In this study, we calculated the dipole position using the following methods to reduce the influence of the MCG signal noise and the heart volume conductor, which generally needs to be described by a heart-torso model.[19–23]

2.2. The extrema circle in the magnetocardiogram

We defined an extrema circle, whose diameter is equal to the distance between the maximum and the minimum value positions in a magnetic field map (MFM). Ideally, the maximum gradient value is located at the midpoint of a line between the maximum and minimum values of the simulated MFM shown in Figs. 1(a) and 1(b). However, due to the influence of data interpolation or measurement error, the maximum gradient value sometimes appears on the boundary of the actual MCG maps, as shown in Figs. 1(c) and 1(d). Therefore, we chose only the maximum gradient value, indicated by an asterisk, in the extrema circle of Fig. 1 for source reconstruction. By using the maximum values $(x_{\max},y_{\max})$ and the maximum gradient values $(x_{m\max},y_{m\max})$ of the field, the dipole parameter (x_0,y_0,z_0) in Eq. (2) can be expressed as[24]

$$\begin{cases} x_0 = x_{m\max}, \\ y_0 = y_{m\max}, \\ z_0 = \sqrt{2}\cdot\sqrt{(x_{m\max}-x_{\max})^2+(y_{m\max}-y_{\max})^2}. \end{cases} \tag{6}$$

The validity of this approach has been demonstrated in simulation, where the accuracy of dipole source localization depends on the resolution of the MFM or the number of measurement sites.

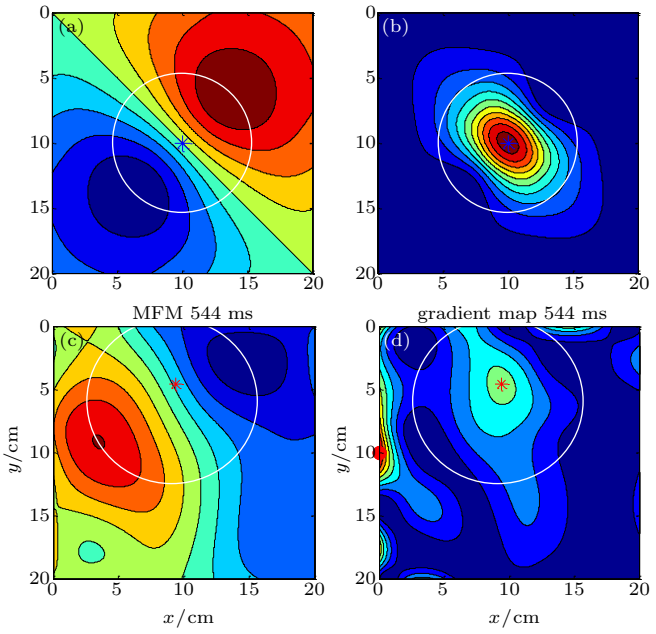


Fig. 1. (color online) The simulated MFM and corresponding gradient map are shown in panels (a) and (b). The MCG map and the corresponding gradient map regarding the MCG data at 544 ms are shown in panels (c) and (d), where the red spot • indicates the position of the maximum gradient value, and the red asterisk ∗ indicates that of the maximum gradient value within the extrema circle.

3. Results

3.1. MCG data

In the following studies, we compute the equivalent current dipole parameters using two sets of real MCG data from a

CRBBB subject and a CLBBB subject, as shown in Figs. 2 and 3. The data were recorded by a four-channel low-temperature SQUID system at Shanghai Ruijin hospital, and the sampling frequency of the signal was 1 kHz.

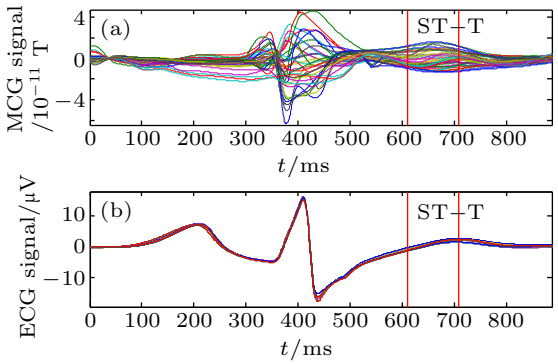


Fig. 2. (color online) The measured MCG (a) and ECG (b) signals of a CRBBB subject at ST–T intervals.

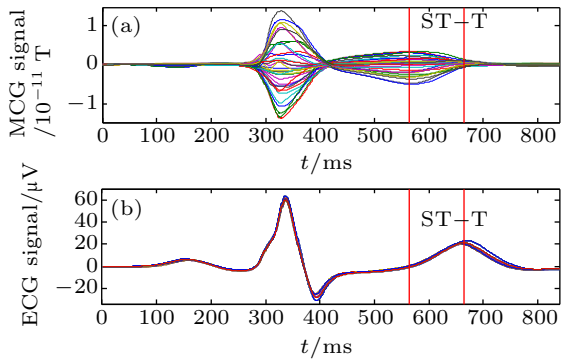


Fig. 3. (color online) The measured MCG (a) and ECG (b) signals of a CLBBB subject at ST–T intervals.

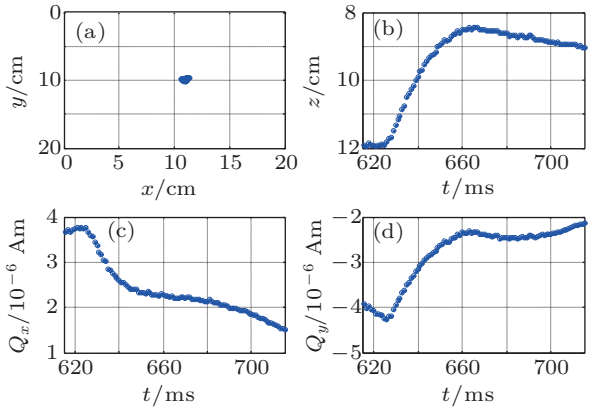


Fig. 4. (color online) The equivalent dipole source parameter curves for the CRBBB subject from 615 ms to 714 ms over a T wave interval: (a) the corresponding time-dependent equivalent dipole location curve on the measurement plane, (b) the dipole depth curve, and (c) and (d) two time-dependent dipole moment component curves.

The reconstructed equivalent dipole source parameters of two subjects during the first 100 ms before the peak of the T wave are shown in Figs. 4 and 5. The corresponding time-dependent equivalent dipole location curve (upper left), the dipole depth curve (upper right), and two time-dependent dipole moment component curves (lower left and lower right) are plotted on the measurement plane in panels (a)–(d), respectively. It is shown in panel (a) of Figs. 4 and 5 that the equivalent current dipole moves in a small area at a T wave interval. The dipole depth and dipole moment curves of the two subjects have different characteristics, as shown in panels (b) and (c).

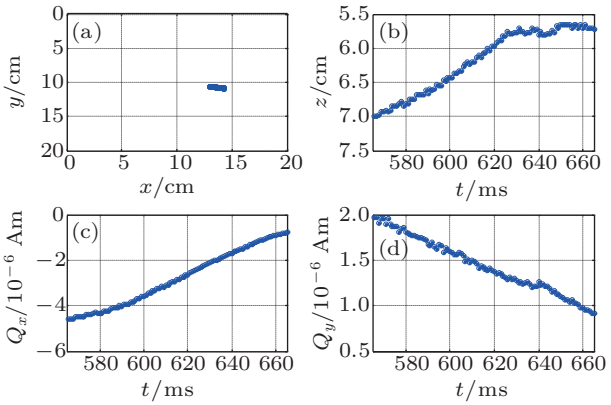


Fig. 5. (color online) The equivalent dipole source parameters of the CLBBB subject from 565 ms to 664 ms over a T wave interval: (a) the corresponding time-dependent equivalent dipole location curve on the measurement plane, (b) the dipole depth curve, and (c) and (d) two time-dependent dipole moment component curves.

3.2. Cardiac electrical activity

Coronal (a) and sagittal (b) MR imaging of a normal heart are shown in Fig. 6. Three dashed ellipses are used to indicate the position of the heart, the left ventricular and the right ventricular in Fig. 6 and Figs. 7 and 8, respectively.

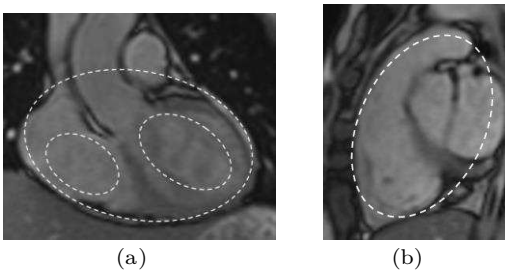


Fig. 6. Diagrammatic sketch of a normal heart in coronal (a) and sagittal (b) MR imaging.

After zooming in on a 5 cm × 5 cm area in Fig. 4(a) or 7(a), the trajectories of the moving single dipole in the QRS interval are seen in Figs. 7(b) and 7(c), respectively, where the QR segment is indicated by green arrows from 364 ms to 410 ms, the RS by red arrows from 411 ms to 437 ms, and that in the T interval is shown by the red arrows from 665 ms to 714 ms in Fig. 7(d). That is to say, the propagation of the electrical excitation from the upper left goes through the lower left to the right side of the heart during the ventricular depolarization of the CRBBB subject.[19] In other words, for a CRBBB subject, the right ventricle contracts later than the left ventricle. The propagation of the electrical excitation from the left ventricle wall to the right ventricle wall during ventricular repolarization is also shown in Fig. 7(d).

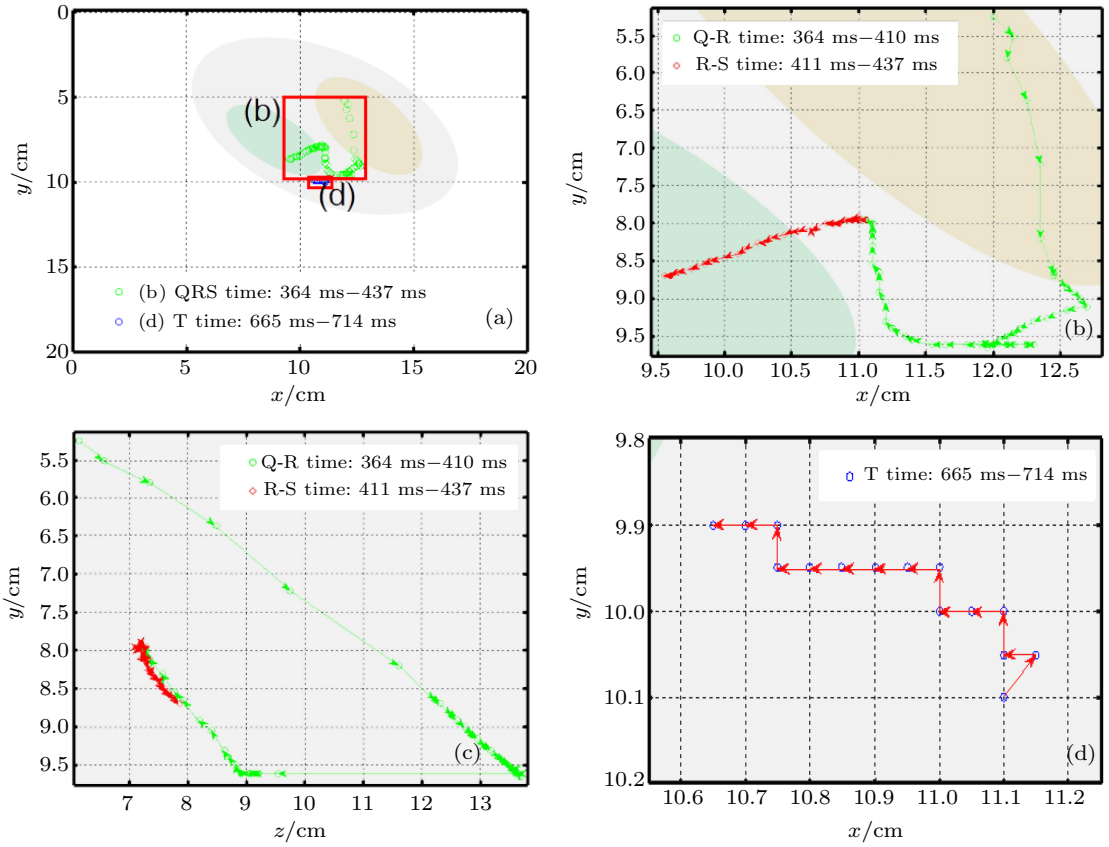


Fig. 7. (color online) (a) The trajectories of the current dipole of a CRBBB subject on the measurement plane, (b) the trajectory during the QRS interval in the *x*–*y* plane, (c) the trajectory during the QRS interval in the *z*–*y* plane, and (d) the trajectory during the T interval.

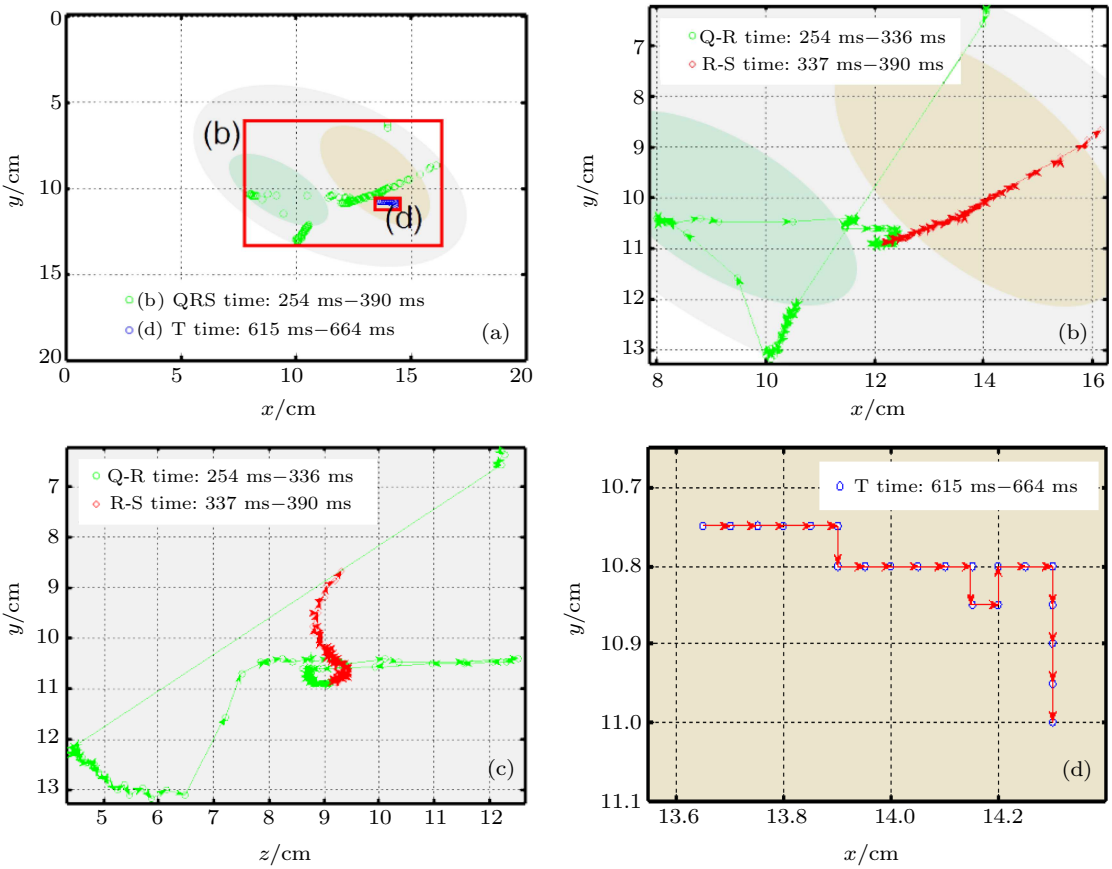


Fig. 8. (color online) (a) The trajectories of the current dipole of a CLBBB subject on the measurement plane, (b) the trajectory during the QRS interval in the *x*–*y* plane, (c) the trajectory during the QRS interval in the *z*–*y* plane, and (d) the trajectory during the T interval.

In Fig. 8, the trajectory of the moving dipole of a CLBBB subject in the QRS interval is seen, as in Fig. 5(a), where QR is indicated by green arrows from 254 ms to 336 ms, RS by red arrows from 337 ms to 390 ms, and that in the T interval is shown by red arrows from 615 ms to 664 ms in panels (b), (c) and (d), respectively. In an area about 5 $\times$ 10 cm^2 on the measurement plane, the direction of the excitation conduction is opposite to that of the CRBBB subject, from the upper left through the lower right to the left side of the heart. In other words, the propagation of the electrical excitation is from the left ventricle wall to the right ventricle wall during ventricular depolarization, as shown in Figs. 8(b) and 8(c); but this is reversed, going from the right ventricle wall to the left ventricle wall during repolarization, as shown in Fig. 8(d).[25]

4. Discussion

4.1. Results and analysis

We calculated six sets of MCG data, including three with CRBBB and another three with CLBBB, and obtained results that are similar to Figs. 7 and 8, respectively.

The source localization accuracy of this method depends on the maximum value of magnetic signals in measurement sites, which can be refined usefully through data interpolation. Since the maximum value and the maximum gradient value in the measurement sites could reflect the effect of a heart volume conductor, this method is used to improve the source localization accuracy in the case of the lack of an acceptable heart-torso model.

4.2. Comparison with the current density map

The pseudo-current density (PCD) map is a well-known tool for clinical diagnosis of cardiac disease.[26–30] The pseudo-current distribution of the heart is calculated based on the gradient estimation of the z component of the magnetic field on the measurement plane.[19]

The trajectories of the maximum pseudo-current during the 100 ms of the T wave from a CRBBB subject or a CLBBB subject are compared with those of the reconstructed moving current dipole in Figs. 9(a) and 9(b), respectively, where green (corresponding to the first 50 ms) and red (the later 50 ms) arrows are the trajectories of the current dipole on the measurement plane. The black arrows represent the magnitude and direction of the dipole moment, and the blue ones are those of the maximum PCD.

We noted that the black and blue arrows in Figs. 9(a) and 9(b) remain a related certain phase at a T wave interval, which may be due to the maximum PCD and the equivalent current dipole at different depths. The phases of the black arrows for the CRBBB subject are clearly larger than those of the blue ones, as shown in Fig. 9(a). This also shows that the diastolic times of the left and right ventricle of the CRBBB patient are asynchronous, since the excitatory propagation of the right ventricle is prolonged and the electrical activity is delayed.

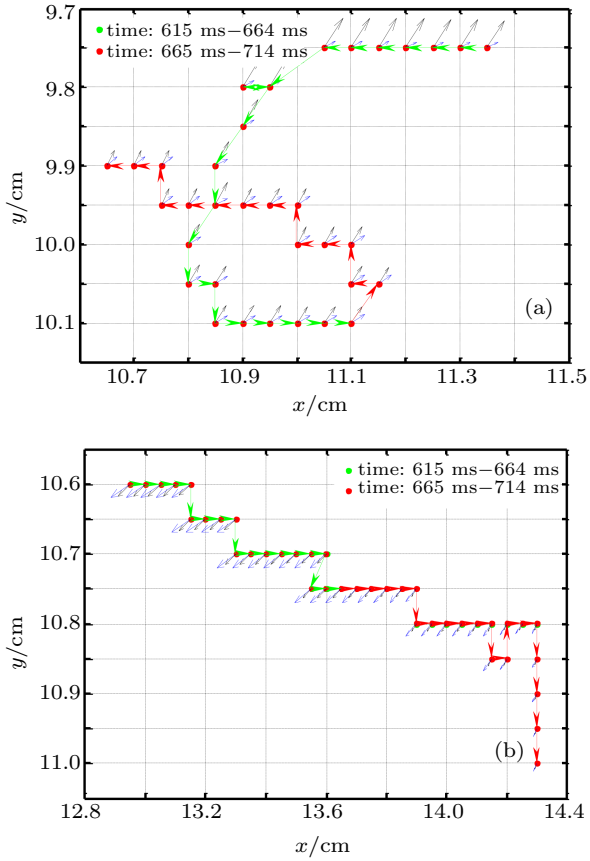


Fig. 9. (color online) The trajectories of the moving current dipole from a CRBBB subject (a) and a CLBBB subject (b) in 100 ms of the T wave. The black arrows represent the magnitude and direction of the dipole moment, and the blue ones those of the maximum current density.

5. Conclusion

A new method to visualize the cardiac electrical activity of CRBBB or CLBBB patients is presented, in which the parameters of an equivalent moving current dipole are expressed by the maximum value and the maximum gradient value in magnetocardiograms. This will be useful in improving source localization accuracy.

The results of two sets of MCG data from CRBBB and CLBBB subjects demonstrated that their dipole parameters in the QRS and T intervals provide useful information for differentiating CRBBB and CLBBB subjects.

We also show the possibility of imaging the excitation conduction in a CRBBB or CLBBB subject during de- and repolarization through the trajectory of the reconstructed equivalent dipole combined with their MCG data. This method will require further evaluation by means of statistical analysis and clinical research.

Acknowledgments

The authors would like to express their gratitude to the Shanghai Institute of Microsystem and Information Technol-

ogy, the Chinese Academy of Sciences, China and especially to professors Zhang Yi, Xie Xiao-Ming and their team for technical assistance. We are also grateful to Shanghai Ruijin Hospital for allowing us to use their MCG data.

References

[1] Cohen D and Hosaka H 1976 *Journal of Electrocardiology* **9** 409
[2] Ma P, Yao K and Xie F X 2005 *Acta Phys. Sin.* **51** 224 (in Chinese)
[3] Gao J, Yang T, Ma P and Dai Y D 2010 *Chin. Phys. B* **19** 067402
[4] Barber M R and Fischmann E J 1961 *Nature* **192** 141
[5] Mirvis D M, Keller F W, Ideker R E, Cox J W Jr., Zettergren D G and Dowdie R F 1977 *J. Electrocardiology* **10** 347
[6] Gulrajani R M and Roberge F A 1984 *IEEE Trans. Biomedical Engineering* **12** 903
[7] Bin H and Dongsheng W 2001 *IEEE Trans. Information Technology in Biomedicine* **5** 181
[8] He B 2004 *Modeling and Imaging of Bioelectrical Activity* (New York: Kluwer Academic/Plenum Publisher) ISBN: 0-306-48112-X
[9] Nenonen J, Purcell C J, Horacek B M, Stroink G and Katila T 1991 *IEEE Trans. Biomed. Eng.* **38** 648
[10] Nenonen J, Katila T, Leinio M, Montonen J, Makijarvi M and Siltanen P 1991 *IEEE Trans. Biomed. Eng.* **38** 658
[11] Weismüller P, Abraham-Fuchs K, Schneider S, Richter P, Kochs M and Hombach V 1992 *Eur. Heart. J.* **13** 616
[12] Nenonen J, Montonen J and Koskinen R 2003 *Int. J. Bioelectromagnetism* **5** 98
[13] Primin M and Nedayvoda I 2009 *International J. Appl. Electromagn. Mech.* **29** 65
[14] De Mehlis M, Tanaka K and Uchikawa Y 2010 *IEEE Trans. Magn.* **46** 1203
[15] Leder U, Haueisen J, Huck M and Nowak H 1998 *the Lancet.* **352** 1825
[16] Wang Q, Ma P, Lu H, Tang X Z, Hua N and Tang F K 2009 *Chin. Phys. B* **18** 5566
[17] Tang F K, Wang Q, Hua N, Lu H, Tang X Z and Ma P 2011 *Chin. Phys. B* **20** 010702
[18] Sarvas J 1987 *Phys. Med. Biol.* **32** 11
[19] Hosaka H, Cohen D, Cuffin B N and Horace B M 1976 *J. Electrocardiol* **9** 418
[20] Purcell C J, Stroink G and Horacek B M 1988 *IEEE Trans. Biomed. Eng.* **35** 671
[21] Purcell C J and Stroink G 1991 *IEEE Trans. Biomed. Eng.* **38** 82
[22] Tan G A, Brauer F, Stroink G and Purcel C J 1992 *IEEE Trans. Biomed. Eng.* **39** 921
[23] Czapski P, Ramon C, Haueisen J and Huntsman L L 1998 *IEEE Trans. Biomed. Eng.* **45** 1313
[24] Jiang S Q and Shi M W 2011 *Report of the 8th NFSI ICBEM*, Banff, Canada
[25] Macfarlane PW, van Oosterom A, Janse M, Camm J, Kligfield P and Pahlm O 2010 *Comprehensive Electrocardiology*, 2nd edn. (London: Springer)
[26] Miyashita T, Kandori A, Tsukada K, Sato M, Terada Y, Horigome H and Mitsui T 1998 *Proceedings of the 20th Annual International Conference of the IEEE Engineering in Medicine and Biology Society* **20** 520
[27] Kandori A, Kanzaki H, Miyatake K, Hashimoto S, Itoh S, Tanaka N, Miyashita T and Tsukada K 2001 *Medical & Biological Engineering & Computing* **39** 21
[28] Hans Koch 2003 *Feldverteilungen aus der MKG-Vitalitätsstudie* (Berlin: PTB-Physikalisch Technische Bundesanstalt)
[29] Ogata K, Kandori A, Miyashita T, Tsukada K, Nakatani S, Shimizu W, Kanzaki H, Miyatake K, Yamada S, Watanabe S and Yamaguchi I 2006 *The International Journal of Cardiovascular Imaging.* **22** 581
[30] Zheng Y Q, Jiang Z Y and Xiaogu C 2001 *Magnetic Imaging Technology and Clinical Applications* (Beijing: People's Medical Publishing House) ISBN: 7-117-04196-X